

Mössbauer study of amorphous $\text{Fe}_{82}\text{B}_{12}\text{Si}_6$

Hang Nam Ok* and A. H. Morrish

Department of Physics, University of Manitoba, Winnipeg, Manitoba, Canada R3T 2N2

(Received 2 June 1980)

Amorphous $\text{Fe}_{82}\text{B}_{12}\text{Si}_6$ in ribbon form has been investigated over a large temperature range from 2 to 796 K using the Mössbauer technique. The values of the average hyperfine field $H_{\text{hf}}(T)$ show a temperature dependence $[H_{\text{hf}}(T) - H_{\text{hf}}(0)]/H_{\text{hf}}(0) = -B_{3/2}(T/T_F)^{3/2} - C_{5/2}(T/T_F)^{5/2} \dots$, for $T/T_F < 0.8$, indicative of spin-wave excitation. The values of $B_{3/2} = 0.34 \pm 0.05$ and $C_{5/2} = 0.21 \pm 0.05$ have been determined. The quadrupole splitting just above T_F is 0.45 mm/s, whereas the average quadrupole shift below T_F is zero. The implication is that the magnetic hyperfine field is randomly oriented with respect to the electric field gradient. A tension experiment indicates that $\text{Fe}_{82}\text{B}_{12}\text{Si}_6$ exhibits positive magnetostriction. This property in combination with thermal expansion is apparently responsible for the in-plane and out-of-plane anisotropy of a clamped sample observed at high and low temperatures, respectively. The Curie and crystallization temperatures are determined to be $T_F = 658$ K and $T_X = 780$ K, respectively.

I. INTRODUCTION

In the last several years, much interest in ferromagnetic metallic glasses has been generated since such materials were produced in technologically useful ribbon form and their magnetic, mechanical, and chemical properties were known to be suitable as possible engineering materials. Many of their interesting properties have been revealed by Mössbauer spectroscopy.

The Mössbauer spectra of a large variety of amorphous alloys¹⁻³ are very similar and consist of structureless absorption lines that are broadened by distributions of magnetic hyperfine fields and quadrupole and isomer shifts. Various methods²⁻⁵ have been employed to evaluate these distributions from the measured spectra under a number of assumptions that may not always be satisfied in reality. The average magnetic hyperfine field measured at the Fe sites of a number of glassy ferromagnets¹ has been reported to follow a much stronger temperature dependence of $T^{3/2}$ than that of crystalline ferromagnets. Furthermore, the $T^{3/2}$ dependence, characteristic of spin-wave excitations, dominates an exceptionally large temperature range. On the other hand, the average quadrupole shifts^{3,6} are known to be zero below the Curie temperature as a result of random atomic arrangements. Mössbauer spectroscopy has also been employed to monitor the crystallization process^{3,7} and the magnetic anisotropy.^{6,8,9}

In the present work the hyperfine interactions and the magnetic anisotropy in a new amorphous ferromagnet, $\text{Fe}_{82}\text{B}_{12}\text{Si}_6$, have been studied between 2 and 796 K.

II. EXPERIMENTAL

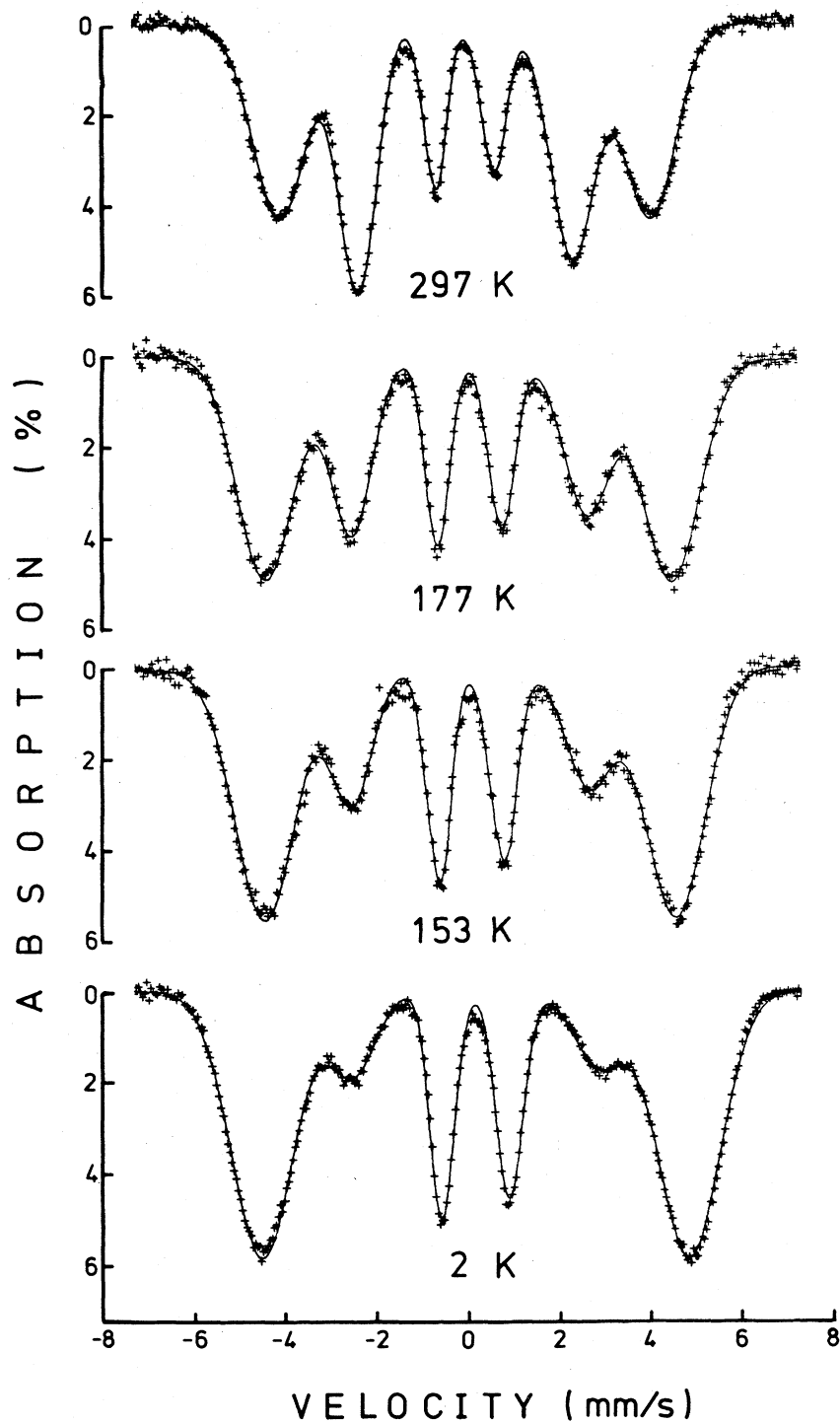
Amorphous $\text{Fe}_{82}\text{B}_{12}\text{Si}_6$ (METGLAS[®] 2605S) in the form of a ribbon 25.4 cm wide and 38 μm thick was obtained from the Allied Chemical Corporation.

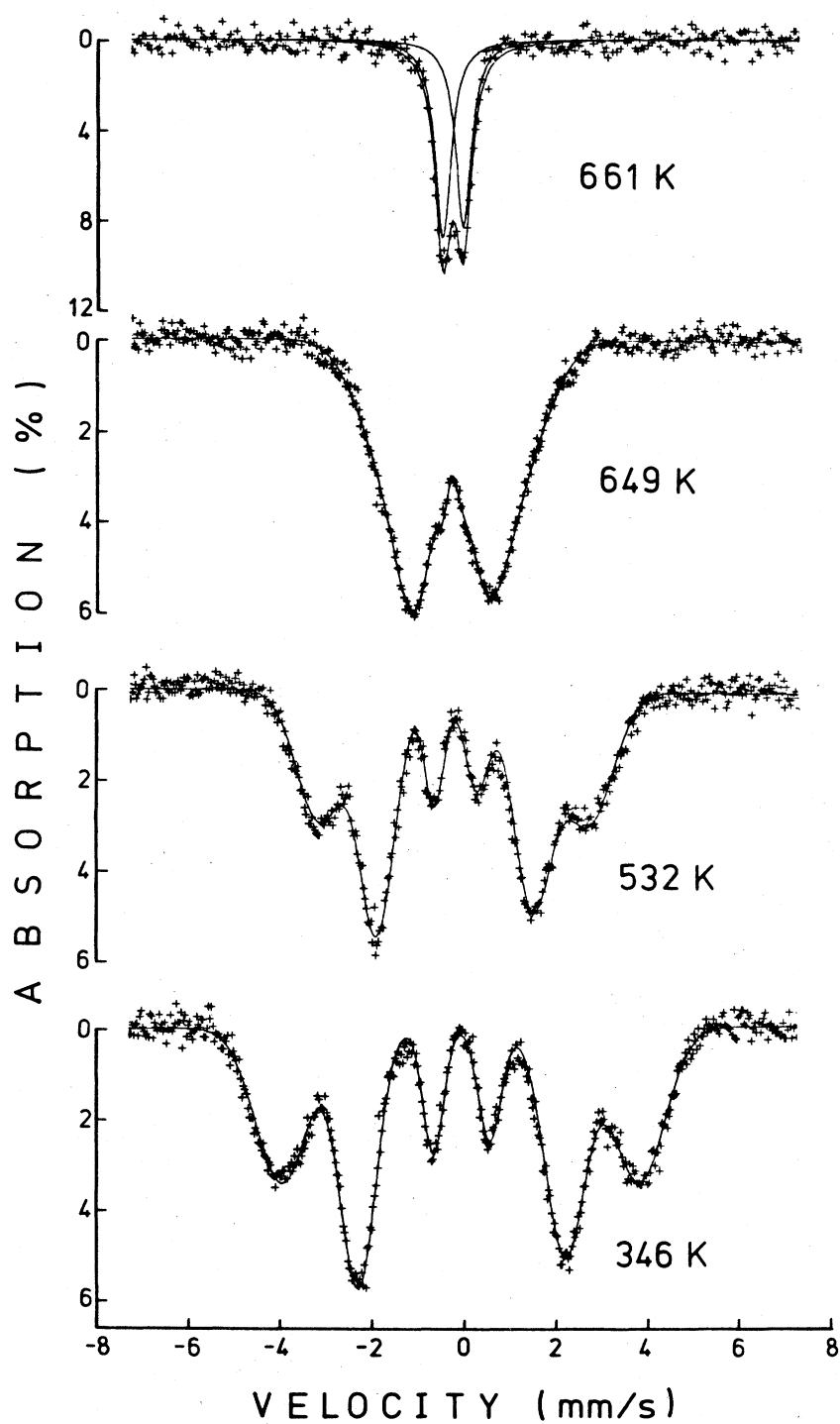
The Mössbauer measurements were performed with an Elscint constant acceleration spectrometer that had linewidths of 0.25 mm/s for the inner lines of a natural iron absorber 12.7 μm thick. The measurements above room temperature were made in a furnace with a temperature stability of 0.5 K. Those below room temperature were obtained in a cryostat with a stability of 0.2 K. For the low-temperature measurements ($T < 300$ K), the sample was clamped between two Be disks with vacuum grease applied on both surfaces of the sample foil. For the measurements at high temperatures ($T > 300$ K), the sample was clamped between two stainless-steel rings with a center-hole of diameter 8 mm. A ^{57}Co source in Rh matrix was used throughout the experiments.

III. RESULTS AND DISCUSSIONS

A. Data analysis

Mössbauer spectra of the as-quenched amorphous $\text{Fe}_{82}\text{B}_{12}\text{Si}_6$ at temperatures below the Curie temperature T_F exhibit broadened six-line patterns as shown in Figs. 1 and 2. This kind of broadened line may be analyzed in terms of a distribution²⁻⁴ of magnetic hyperfine fields assuming that broadening from distributions of quadrupole splittings and isomer shifts is insignificant. However, the quadrupole splitting of

FIG. 1. Mössbauer spectra of $\text{Fe}_{82}\text{B}_{12}\text{Si}_6$ at low temperatures.

FIG. 2. Mössbauer spectra of $\text{Fe}_{82}\text{B}_{12}\text{Si}_6$ at high temperatures.

amorphous $\text{Fe}_{82}\text{B}_{12}\text{Si}_6$ is as large as 0.45 mm/s at 661 K, and then line broadening from the distribution of quadrupole splittings is not negligible as the following analysis will show.

When the quadrupole interaction is much weaker than the magnetic hyperfine interaction, the Mössbauer line shift from the quadrupole interaction can be described by¹⁰

$$E_Q = \frac{1}{8} e^2 q Q (3 \cos^2 \theta - 1 + \eta \sin^2 \theta \cos 2\phi) \quad (1)$$

where θ and ϕ are the angles, in polar coordinates, between the magnetic hyperfine field vector and the principal axes of the electric-field-gradient tensor. On assuming that the maximum electric field gradient q and the asymmetry parameter η are independent of θ and ϕ , the average value of E_Q taken over all directions vanishes; viz.

$$\begin{aligned} \langle E_Q \rangle &= \frac{1}{4\pi} \int_0^\pi \int_0^{2\pi} \frac{1}{8} e^2 q Q (3 \cos^2 \theta - 1 + \eta \sin^2 \theta \cos 2\phi) \\ &\quad \times \sin \theta \, d\theta \, d\phi \\ &= 0 \end{aligned} \quad (2)$$

However, the line broadening from this random distribution is not zero; that is,

$$\begin{aligned} 2\Delta E_Q &= 2[(\langle E_Q^2 \rangle)^{1/2}] \\ &= 2(\langle E_Q^2 \rangle)^{1/2} \\ &= 2 \left[\frac{1}{4\pi} \int_0^\pi \int_0^{2\pi} \frac{e^4 q^2 Q^2}{64} \right. \\ &\quad \left. \times (3 \cos^2 \theta - 1 + \eta \sin^2 \theta \cos 2\phi)^2 \sin \theta \, d\theta \, d\phi \right]^{1/2} \\ &= \frac{1}{\sqrt{5}} \frac{e^2 q Q}{2} (1 + \frac{1}{3} \eta^2)^{1/2} \\ &= \frac{1}{\sqrt{5}} 0.45 \\ &= 0.20 \text{ mm/s} \end{aligned}$$

Another source of broadening can be estimated from the linewidth, 0.42 mm/s, of the quadrupole doublet above the Curie temperature. In view of the 0.25-mm/s linewidth of an iron foil, a line-broadening of ~ 0.17 mm/s of the doublet is the result of distributions of the isomer shift and magnitudes of q and η in addition to the thickness effect of the absorber. Thus, the combined broadening from distributions of quadrupole splitting and isomer shift including broadening from the thickness effect amounts to as large as about 0.37 mm/s below T_F , whereas the linewidths of the six absorption lines at room tem-

perature are 1.38, 0.97, 0.59, 0.66, 1.11, and 1.38 mm/s.

Distributions of the quadrupole splitting and the isomer shift, in addition to the distribution of the magnetic hyperfine field, can be attempted with some additional assumptions.⁵ However, the reliability of such analysis is undoubtedly limited. In the present analysis, no attempt was made to get the distribution functions, and only average values were obtained by fitting six Gaussian lines to the Mössbauer spectra. The reason why Gaussian line shapes were used instead of the usual Lorentzian line shapes was based on the result² that when the broadened absorption lines of amorphous solids were separated by an external magnetic field, Gaussian line shapes gave better fits. In the present fit, lines symmetrically located in a six-line pattern are assumed to have the same areas. The average values of the magnetic hyperfine field, quadrupole splitting, and isomer shift were obtained from least-squares fits, and are shown in Figs. 3 through 5.

B. Magnetic hyperfine fields

Figure 3 shows the fractional change of the magnetic hyperfine field, $[H_{\text{hf}}(T) - H_{\text{hf}}(0)]/H_{\text{hf}}(0)$, as a function of T . For most amorphous ferromagnets¹ investigated so far, the magnetic hyperfine field decreases with increasing temperature according to

$$\frac{H_{\text{hf}}(T) - H_{\text{hf}}(0)}{H_{\text{hf}}(0)} = -B_{3/2} \left(\frac{T}{T_F} \right)^{3/2} - C_{5/2} \left(\frac{T}{T_F} \right)^{5/2} \quad (3)$$

The temperature dependence of the leading term has its origin in the excitations of long-wavelength spin waves for which the detailed atomic arrangements are not important.¹¹ A least-squares fit of Eq. (3) to the magnetic hyperfine field data gave $B_{3/2} = 0.34 \pm 0.05$ and $C_{5/2} = 0.21 \pm 0.05$. This value of $B_{3/2}$ for the

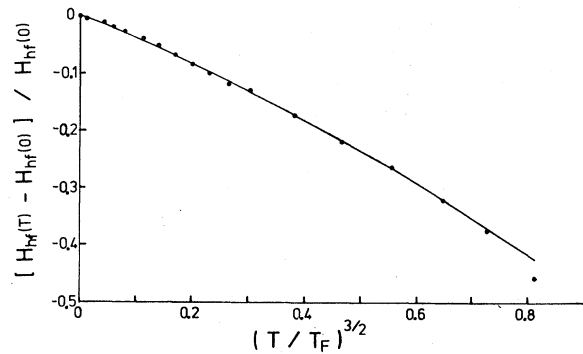


FIG. 3. Fractional change of the magnetic hyperfine field, H_{hf} , as a function of $(T/T_F)^{3/2}$.

amorphous ferromagnet, $\text{Fe}_{82}\text{B}_{12}\text{Si}_6$, is much larger than those of crystalline ferromagnets¹² such as α -Fe and Ni; $B_{3/2} = 0.12$ for Ni and $B_{3/2} = 0.11$ for α -Fe. Apparently, more spin waves of long wavelengths are excited in amorphous ferromagnets than in crystalline ferromagnets.

Alternatively, it may be noted that the data of Fig. 3 can be fitted with only the $(T/T_F)^{3/2}$ term by using different values for $B_{3/2}$ above and below $T \approx 150$ K. For $T < 150$ K, $B_{3/2} \approx 0.36$, whereas for $T > 150$ K, $B_{3/2} \approx 0.57$. Whether this approach implies that the amorphous nature of the material leads to a discontinuous change in $B_{3/2}$ at certain temperatures or not is problematical at this time.

C. Quadrupole splittings

Figure 4 shows the temperature-dependence of the quadrupole splitting of $\text{Fe}_{82}\text{B}_{12}\text{Si}_6$. Above the Curie temperature, T_F , the quadrupole splitting is given by

$$\epsilon = \frac{1}{2} e^2 q Q (1 + \frac{1}{3} \eta^2)^{1/2} .$$

The value of ϵ was found to be 0.45 mm/s at 661 K which is just above T_F . On the other hand, below T_F , ϵ has been calculated from the positions of Mössbauer absorption lines from the expression

$$\epsilon = \frac{1}{2} (V_6 - V_5 + V_1 - V_2) ,$$

where V_i represents the position of the i th absorption line in mm/s. ϵ is related to E_Q of Eq. (1) by

$$\epsilon = 2 \langle E_Q \rangle . \quad (4)$$

Figure 4 shows that, within experimental errors, all ϵ values are zero below T_F . This, in turn, means from Eqs. (2) and (4) that the average value of the quadrupole shift over all directions is zero. In other words, the magnetic-hyperfine field is randomly oriented with respect to the principal axes of the electric field gradient.

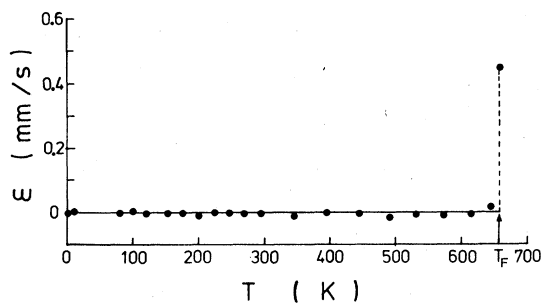


FIG. 4. Temperature dependence of the quadrupole shift ϵ .

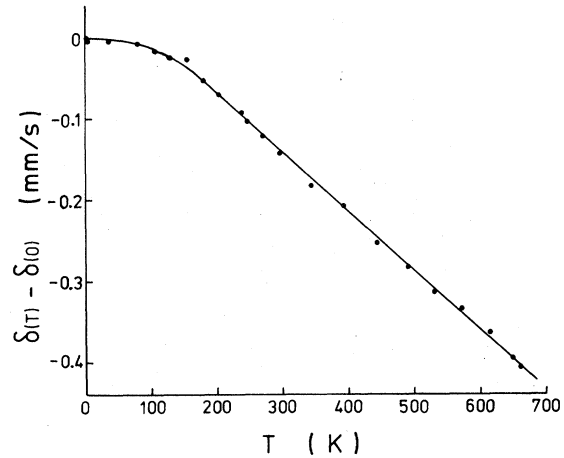


FIG. 5. Temperature dependence of the isomer shift δ .

D. Isomer shifts

Figure 5 shows the temperature dependence of the isomer shift; a linear variation can be seen above about 150 K. This kind of temperature dependence is known to be the result of the second-order Doppler shift. If the forces coupling the atoms are assumed to be harmonic, the temperature-dependent shift¹³ is linear with respect to T at high temperatures and the slope is given by

$$\frac{d\delta(T)}{dT} = -\frac{3kE_\gamma}{2Mc^2} ,$$

where k is Boltzmann's constant, M is the atomic mass, and E_γ is the γ -ray energy. For the 14.4-keV γ ray of ^{57}Fe , this slope is calculated to be -0.000731 mm/s K. The solid line above 150 K in Fig. 5 is drawn with this slope, and is in good agreement with the experimental values. This suggests that the forces coupling the atoms in amorphous $\text{Fe}_{82}\text{B}_{12}\text{Si}_6$ are harmonic to a good approximation.

E. Magnetic anisotropy

Information about the directions of the magnetic moments can be obtained from the relative intensities of the Mössbauer absorption lines. For the 14.4-keV γ rays of ^{57}Fe , the relative intensity ratio of the second to the first or the fifth to the sixth lines is given by

$$\frac{A_{2,5}}{A_{1,6}} = \frac{4 \sin^2 \theta}{3(1 + \cos^2 \theta)} \quad (5)$$

where θ is the angle between the γ ray and the direction of the magnetic hyperfine field. The ratio $A_{2,5}/A_{1,6}$ varies from 0 to $\frac{4}{3}$ as θ changes from 0 to

90°. Figure 6 shows the area ratio $A_{2,5}/A_{1,6}$ as a function of temperature.

Above room temperature this ratio increases with increasing temperature and reaches the theoretical maximum value of 1.33 above about 450 K. In other words, the magnetic moments are parallel to the foil plane of the sample. Similar in-plane anisotropy has been observed for amorphous $\text{Fe}_{80}\text{P}_{16}\text{BC}_3$ (Ref. 14) and $\text{Fe}_{78}\text{B}_{12}\text{Si}_{10}$ (Ref. 6) ribbons.

In order to determine whether this property has anything to do with clamping, a small sample of diameter 8 mm was placed in an unclamped state in a cavity consisting of two Be plates and an aluminum annular ring. The Mössbauer spectra taken for this unclamped sample show that the areal ratio $A_{2,5}/A_{1,6}$ is nearly independent of temperature, as indicated by the symbols \times in Fig. 6. Thus, the increase of $A_{2,5}/A_{1,6}$ for the clamped sample with increasing temperature is not intrinsic to the material but is caused by some external stress. The external stress may have its origin in the difference between the linear expansion coefficients of the amorphous material and the clamping rings. The value of the thermal linear expansion coefficient of $\text{Fe}_{82}\text{B}_{12}\text{Si}_6$ is not known, but that¹⁵ of the amorphous $\text{Fe}_{83}\text{B}_{17}$, which has a similar composition, is zero in the temperature range 300 to 620 K. If the thermal-expansion coefficient¹⁶ $1.40 \times 10^{-5} \text{ K}^{-1}$ of the stainless-steel rings is assumed to be larger than that of the amorphous $\text{Fe}_{82}\text{B}_{12}\text{Si}_6$, the clamping rings can exert increasing radial tension in the ribbon plane of the amorphous sample with increasing temperature, thereby making the ribbon plane magnetically easy if the $\text{Fe}_{82}\text{B}_{12}\text{Si}_6$ is positively magnetostrictive.

In order to clarify this point, an external tension was applied along a direction of the ribbon plane of the sample at room temperature while Mössbauer

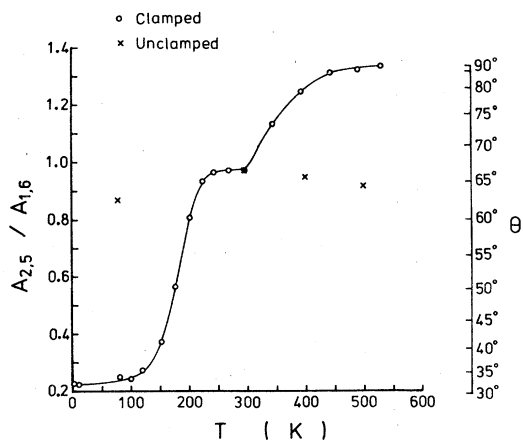


FIG. 6. The areal ratio $A_{2,5}/A_{1,6}$ of the absorption lines 2 and 5 to the outer lines 1 and 6 as a function of temperature. The average canting angle, θ , is also shown.

spectra were collected. As shown in Fig. 7, the areal ratio $A_{2,5}/A_{1,6}$ increases with increasing tensile stress, demonstrating that the magnetostriction is positive. Since the tensile stress is proportional to the fractional increase in length within the elastic limit, and also the fractional increase in length from thermal expansion is proportional to the increase in temperature, both the tension and the temperature dependences of the areal ratio $A_{2,5}/A_{1,6}$ should be proportional to each other provided that the temperature dependence of the magnetostriction is neglected in the temperature region 300–500 K. To aid comparison, the high-temperature portion of Fig. 6 is transferred to Fig. 7 in such a way that the saturation values of both curves coincide. The two curves are the same within the experimental errors, demonstrating that the tensile stress from the difference of thermal expansion coefficients is the origin of the in-plane anisotropy observed for the clamped sample above room temperature.

On the other hand, the value of $A_{2,5}/A_{1,6}$ at low temperatures decreases rapidly below 225 K, showing an out-of-plane anisotropy. However, this anisotropy is also caused by external stress, because the cavity-type experiment of 80 K showed no such effect as shown in Fig. 6. For the low-temperature measurements, the sample was sandwiched between two beryllium plates with vacuum grease. Similar out-of-plane anisotropy has been observed for amorphous $\text{Fe}_{40}\text{Ni}_{40}\text{P}_{14}\text{B}_6$ (Refs. 8 and 9) and $\text{Fe}_{80}\text{B}_{20}$ (Ref. 3) sandwiched between thin aluminum foils with vacuum grease.

The freezing point of our vacuum grease was determined to be $220 \pm 5 \text{ K}$. Since the vacuum grease is expected to have a much larger thermal expansion coefficient⁹ than the amorphous sample, compressive stresses just opposite to those at high temperatures are exerted on the sample below about

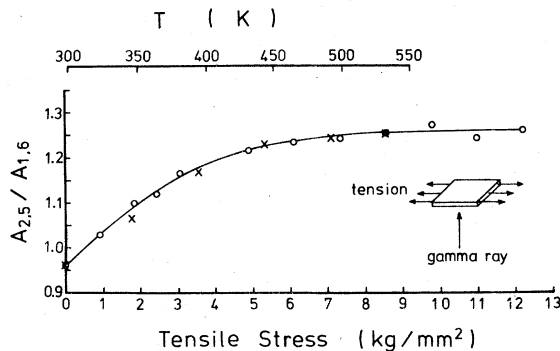


FIG. 7. The room-temperature areal ratio $A_{2,5}/A_{1,6}$ of the absorption lines 2 and 5 to the outer lines 1 and 6 as a function of tensile stress, shown as circles. The points \times are transferred from the portion of Fig. 6 above room temperature.

220 K, thus rotating the easy axis out of the ribbon plane through the positive magnetostriction.

F. Curie and crystallization temperatures

In order to determine the Curie temperature T_F and crystallization temperature T_X , the velocity transducer of the Mössbauer spectrometer was set at zero velocity (the zero velocity corresponds to the line position of the higher-velocity component of the quadrupole doublet just above T_F) and counts were recorded for a fixed counting time of 30 s while the temperature was raised at a rate of 200 K/h from 300 to 796 K. The results are shown in Fig. 8.

At the disappearance of magnetic ordering, the count rate is expected to show a rapid decrease. From the graph the Curie temperature is determined to be 658 ± 2 K. As the temperature was further increased, the count rate increased slowly due to the second-order Doppler effect and partial crystallization, and then increased suddenly at 780 K. This behavior results because the amorphous state is rapidly crystallizing and the Curie temperatures of the crystalline phases are higher than 780 K. After the amorphous $\text{Fe}_{82}\text{B}_{12}\text{Si}_6$ has reached the crystallization temperature $T_X = 780 \pm 2$ K, the amorphous state has

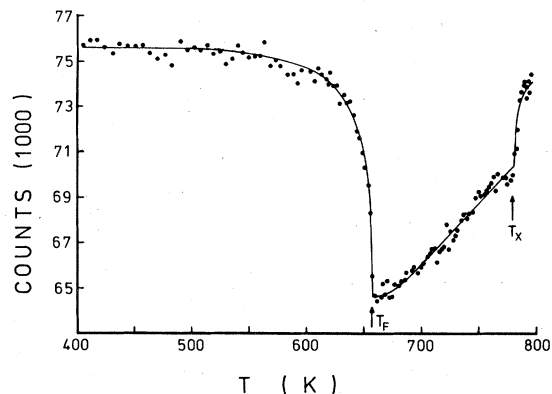


FIG. 8. Counts measured for 30 s at zero Doppler velocity as a function of temperature. The heating rate was 200 K/h.

been completely transformed into crystalline phases. Confirmation was obtained by taking a Mössbauer spectrum and an x-ray-diffraction pattern after cooling down the sample to room temperature. Figure 9 shows the Mössbauer spectrum of the sample taken at room temperature right after the second transition of Fig. 8 is completed. The analysis of this spectrum

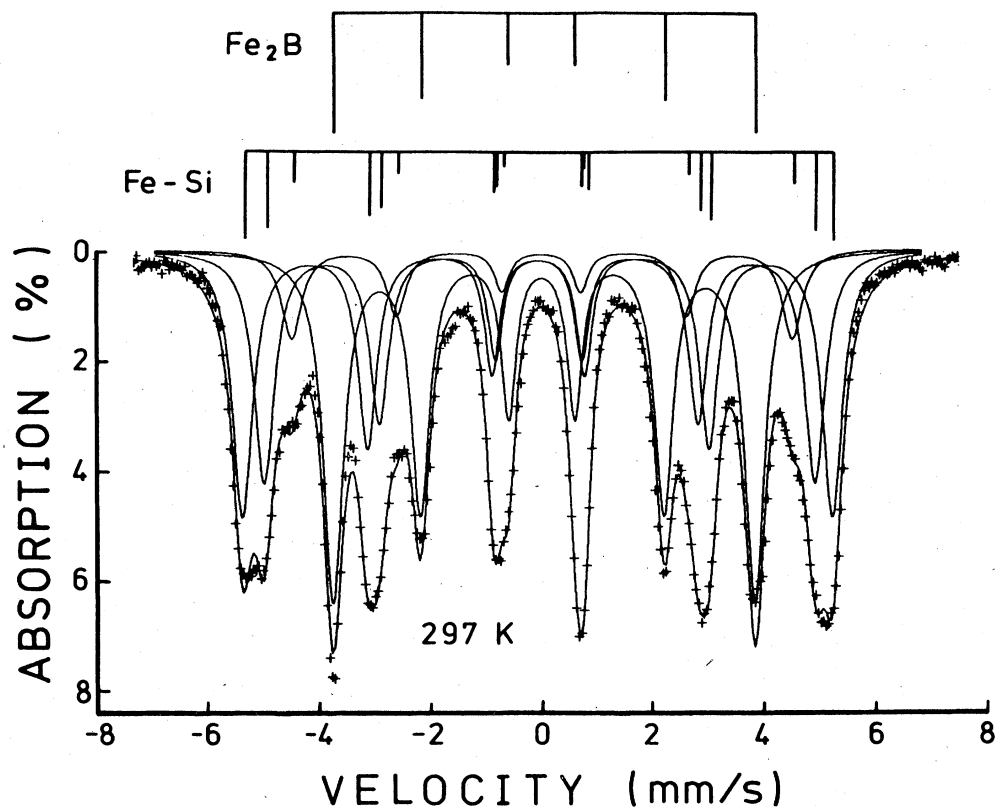


FIG. 9. Mössbauer spectrum taken at room temperature immediately after completion of the second transition T_X in Fig. 8.

shows that the crystalline phases¹⁷ are Fe₂B and Fe-9 at. % Si alloy.

IV. CONCLUSIONS

The amorphous state of ferromagnetic Fe₈₂B₁₂Si₆ has been studied by ⁵⁷Fe Mössbauer spectroscopy from 2 to 796 K, and the following results are obtained.

At low temperatures the values of the magnetic hyperfine field $H_{\text{hf}}(T)$ show a $T^{3/2}$ dependence that is related to the preferential excitation of long-wavelength spin waves. The $T^{3/2}$ coefficient is larger than that of crystalline ferromagnets. The random orientation of the magnetic hyperfine field with respect to the electric field gradient below T_F results in a vanishing average quadrupole shift and line broadening of 0.20 mm/s, whereas the quadrupole splitting just above T_F is measured to be 0.45 mm/s. The tem-

perature dependence of the isomer shift is linear above 150 K and has a slope consistent with the harmonic nature of the atomic binding forces.

The tension experiment indicates that amorphous Fe₈₂B₁₂Si₆ is highly magnetostrictive with a positive magnetostriction constant. This property is found to rotate the magnetic moments when external stresses are caused by thermal expansion or contraction, even though the magnetic anisotropy under no stress is nearly independent of temperature.

The Curie and crystallization temperatures are determined to be $T_F = 658$ K and $T_X = 780$ K, respectively, for the heating rate of 200 K/h. Examination of a Mössbauer spectrum taken right after completion of crystallization shows that the crystalline products are Fe₂B and Fe-9 at. % Si alloy.

Financial support for this research was provided by the Natural Sciences and Engineering Research Council of Canada.

*On leave from Dept. Phys., Yonsei University, Seoul, Korea.

¹C. L. Chien and R. Hasegawa, Phys. Rev. B **16**, 2115 (1977).

²P. J. Schurer and A. H. Morrish, Solid State Commun. **28**, 819 (1978).

³C. L. Chien, Phys. Rev. B **18**, 1003 (1978).

⁴B. Window, J. Phys. E **4**, 401 (1971).

⁵J. Vincze, Solid State Commun. **25**, 689 (1978).

⁶P. J. Schurer and A. H. Morrish, Phys. Rev. B **20**, 4660 (1979).

⁷T. Kemény, I. Vincze, and B. Fogarassy, Phys. Rev. B **20**, 476 (1979).

⁸C. L. Chien and R. Hasegawa, J. Appl. Phys. **47**, 2234 (1976).

⁹A. M. van Diepen and F. J. A. den Broeder, J. Appl. Phys. **48**, 3165 (1977).

¹⁰Hang Nam Ok and J. G. Mullen, Phys. Rev. **168**, 563

(1968); Hang Nam Ok and B. J. Evans, Phys. Rev. B **14**, 2956 (1976).

¹¹C. Herring and C. Kittel, Phys. Rev. **81**, 869 (1951).

¹²B. E. Argyle, S. H. Charap, and E. W. Pugh, Phys. Rev. **132**, 2051 (1963).

¹³B. D. Josephson, Phys. Rev. Lett. **4**, 341 (1960).

¹⁴C. L. Chien and R. Hasegawa, IEEE Trans. Magn. **12**, 951 (1976).

¹⁵K. Fukamichi, M. Kikuchi, S. Arakawa, and T. Masumoto, Solid State Commun. **23**, 955 (1977).

¹⁶Y. S. Touloukian, R. K. Kirby, R. E. Taylor, and P. D. Desai, *Thermal Expansion* (Plenum, New York, 1975), p. 1138.

¹⁷Hang Nam Ok and A. H. Morrish, Phys. Rev. B **22**, 3471 (1980).